

# The relation between the statistics of open ocean currents and the temporal correlations of the wind

Golan Bel<sup>1,\*</sup> and Yosef Ashkenazy<sup>1,†</sup>

*<sup>1</sup>Department of Solar Energy and Environmental Physics,  
Blaustein Institutes for Desert Research,  
Ben-Gurion University of the Negev, Sede Boqer Campus 84990, Israel*

## Abstract

We study the statistics of wind-driven open ocean currents. Using the Ekman layer model for the integrated currents, we investigate, analytically and numerically, the relation between the wind distribution and its temporal correlations and the statistics of the open ocean currents. We find that temporally long-range correlated wind results in currents whose statistics is proportional to the wind-stress statistics. On the other hand, short-range correlated wind leads to Gaussian distributions of the current components, regardless of the stationary distribution of the winds, and therefore, to a Rayleigh distribution of the current amplitude if the wind stress is isotropic. An interesting result is the existence of an optimum in the amplitude of the ocean currents as a function of the correlation time of the wind stress. The results were validated using an oceanic general circulation model.

PACS numbers: 92.60.Cc, 91.10.Vr, 88.05.Np, 92.60.Gn

Ocean currents are generated by local and remote forces/factors, including winds, tides, buoyancy fluxes and various types of waves. While many studies have investigated the distribution of the wind over land [1–3], focusing on its relevance to energy production, the distribution of ocean currents has received much less attention [4]. Moreover, currently there is no accepted theory explaining the observed statistics of surface ocean currents. Here, we propose a simple physical theory for the distribution of wind-driven ocean currents and its relation to the spatially variable temporal correlations of the wind (see Fig. 1). We show that the distribution of wind-driven ocean currents strongly depends on the temporal correlations of the wind—when the wind exhibits long-range temporal correlations, the ocean current statistics is proportional to the wind-stress statistics, while for short-range correlations of the wind, the different components of the current vector follow Gaussian distributions. It was previously reported that the probability density function (PDF) of ocean currents follows the Weibull distribution [4–8]—we argue that this is not necessarily the case, even if the wind-stress magnitude follows the Weibull distribution [9].

Oceans play a major and important role in the climate system, and ocean circulation underlies many climate phenomena, from scales of meters to thousands of kilometers and from scales of minutes to decades. The gap in our understanding of ocean current statistics leads to a lack in the understanding of the statistics of other related climate variables. Filling in this gap will be useful in many fields: it may help to predict extreme current events and, thus, may help to securely design maritime-associated structures. In light of the increasing efforts to find alternative sources of energy and the idea of using ocean currents as such a source, knowledge of the currents' PDF may help to better estimate the energy production and to appropriately design ocean current turbines that will withstand even extreme current events. Moreover, knowledge regarding current statistics and, in particular, its relation to the wind-stress statistics may improve the parametrization of small-scale processes in state-of-the-art general circulation models (GCMs).

The study of wind-driven ocean currents goes back more than 100 years, to the time when Ekman [10] proposed his classical simple model to explain the effect of Earth's rotation on upper ocean currents. His model predicted that the depth-integrated current vector is perpendicular to the wind vector, a prediction that was largely proven by observation. Since then, many studies have used Ekman's model to propose more realistic models for ocean currents as well as for surface winds [11, 12]. In what follows, we use Ekman's model [10] to study the statistics of wind-driven ocean currents.

*The Model:* In spite of the simplicity of the Ekman model, it will enable us to start investigating

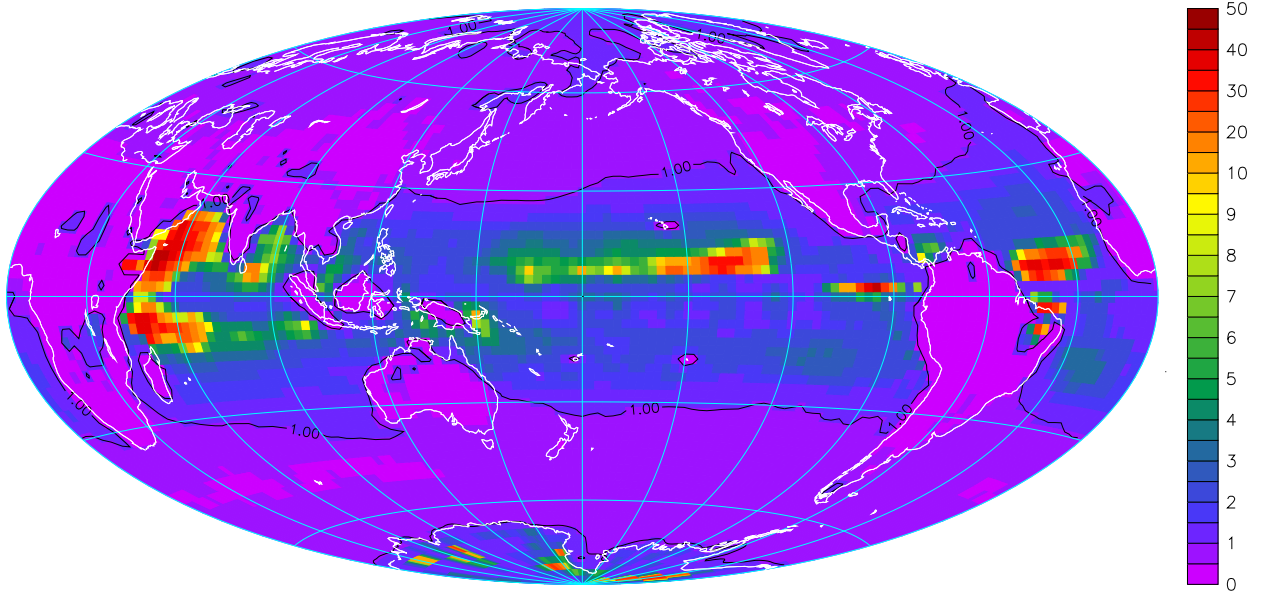


FIG. 1: A map of the correlation time (in days) of the wind-stress magnitude. We define the correlation time as the time at which the normalized auto-correlation function first drops below  $1/e$ . Clearly, there is a large variability in the correlation time. One can also notice the remarkably shorter correlation time overland compared with that over the ocean (except for the polar regions). The map is based on the NCEP/NCAR reanalysis six-hourly wind data for the period of 1993-2010 [13]. The spatial resolution of the data is  $2.5^\circ \times 2.5^\circ$ . Other definitions of the correlation time yield qualitatively the same results. The black contour line indicates a one-day correlation time and the white line indicates the coast line. A grid (light blue lines) of  $30^\circ \times 30^\circ$  was superimposed on the map.

the coupling between the wind stress and the ocean currents. The time,  $t$ , and depth,  $z$ , dependent equations of the Ekman model [10], describing the dynamics of the zonal (east-west)  $U$  and meridional (south-north)  $V$  components of the current vector, are:

$$\begin{aligned}\frac{\partial U}{\partial t} &= fV + \nu \frac{\partial^2 U}{\partial z^2} \\ \frac{\partial V}{\partial t} &= -fU + \nu \frac{\partial^2 V}{\partial z^2},\end{aligned}\tag{1}$$

where  $f = (4\pi/T_d) \sin(\phi)$  is the local Coriolis parameter ( $T_d$  is the duration of a day in seconds and  $\phi$  is the latitude), and  $\nu$  is the eddy viscosity coefficient, assumed to be depth-independent. The boundary conditions are chosen such that the current derivative, with respect to the depth coordinate  $z$ , is proportional to the integrated current at the bottom of the layer described by our

model and to the wind-stress vector  $(\tau_x, \tau_y)$  at the surface [11, 12],

$$\begin{aligned} \frac{\partial U}{\partial z} \Big|_{z=-h} &= \frac{r}{\nu} u(t); & \frac{\partial U}{\partial z} \Big|_{z=0} &= \frac{\tau_x}{\rho_0 \nu}; \\ \frac{\partial V}{\partial z} \Big|_{z=-h} &= \frac{r}{\nu} v(t); & \frac{\partial V}{\partial z} \Big|_{z=0} &= \frac{\tau_y}{\rho_0 \nu}, \end{aligned} \quad (2)$$

where,

$$u \equiv \int_{-h}^0 U(z) dz; \quad v \equiv \int_{-h}^0 V(z) dz. \quad (3)$$

Here, we introduce the following notation:  $h$  is the depth of the upper ocean layer,  $r$  is a proportionality constant representing the bottom drag viscosity (the value used for  $r$  in the numerical calculations is based on the empirical estimate outlined in [14]),  $(\tau_x, \tau_y)$  are the wind-stress components, and  $\rho_0$  is the ocean water density (hereafter assumed to be constant ( $\rho_0 = 1028 \text{ kg/m}^3$ )). By integrating eqs. (1) over a sufficiently deep layer (i.e.,  $h \gg \sqrt{\nu/2f}$ ), we obtain the equations describing the integrated currents and their coupling to the wind stress,

$$\begin{aligned} \frac{\partial u}{\partial t} &= fv - ru + \frac{\tau_x}{\rho_0}, \\ \frac{\partial v}{\partial t} &= -fu - rv + \frac{\tau_y}{\rho_0}. \end{aligned} \quad (4)$$

To allow a simpler treatment of these equations, we define  $w \equiv u + iv$ . It is easy to show that  $w$  obeys the following equation:

$$\frac{\partial w}{\partial t} = -ifw - rw + \frac{\tau}{\rho_0}, \quad (5)$$

where  $\tau \equiv \tau_x + i\tau_y$ . The formal solution of equation (5) is

$$w(t) = w(0)e^{-(if+r)t} + \frac{1}{\rho_0} \int_0^t \tau(t') e^{-(if+r)(t-t')} dt'. \quad (6)$$

This formal solution demonstrates that the currents depend on the history of the wind stress, and therefore, the distribution of the currents depends, not only on the wind-stress distribution, but on all multi-time moments of the wind stress. However, the two extreme limits are quite intuitive. When the correlation time of the wind stress,  $T$ , is long (i.e.,  $T \gg 1/r$  and  $T \gg 1/f$ ), one expects that the currents will be proportional to the wind stress since the ocean has enough time to adjust to the wind and to almost reach a steady state. In terms of eq. (6), in this limit,  $\tau(t')$

can be approximated by  $\tau(t)$  since its correlation time is longer than the period over which the exponential kernel is non-zero. In the other limit, when the correlation time of the wind stress is very short (i.e.,  $rT \ll 1$  and  $fT \ll 1$ ), namely, the wind stress is frequently changing in a random way, the ocean is not able to gain any current magnitude. In this case, the central limit theorem implies that each component of the current vector is Gaussian distributed.

To allow analytical treatment, we proceed by considering two special idealized cases in which the formal solution takes a closed analytical form. For simplicity, we only consider the case of statistically isotropic wind stress, namely,  $\langle \tau_x^n \rangle = \langle \tau_y^n \rangle$  where  $n$  is a positive integer and the different components of the wind stress are independent— $\langle \tau_x^m \tau_y^n \rangle = 0$  where  $m$  and  $n$  are positive integers.

*Step-like wind stress:* A simple way to model the temporal correlations of the wind is by assuming that the wind vector randomly changes every time period  $T$  while remaining constant between the “jumps”. By integrating the solution of  $w$  (eq. (6)) and taking into account the fact that the distribution of  $w$  at the initial time and final time should be identical, one can obtain the expressions for the second and fourth moments (ensemble average over many realizations of the stochastic wind stress) of the current amplitude. To better relate our results to the outcome of data analysis, we also need to consider the time average since the records are independent of the constant wind-stress period. Calculating the double averaged second moment, we get

$$\overline{\langle |w|^2 \rangle} = \frac{\langle |\tau|^2 \rangle \left( 1 + \frac{1-A_1}{rT} - 2 \frac{r(1-A_1)+fA_2}{T(f^2+r^2)} \right)}{(f^2 + r^2) \rho_0^2}, \quad (7)$$

where we have introduced the notations  $A_1 \equiv \exp(-rT) \cos(fT)$  and  $A_2 \equiv \exp(-rT) \sin(fT)$ . The two extreme limits discussed earlier can be easily realized and understood. When the correlation time  $T$  is very long compared with  $1/r$ , the second moment of the current is proportional to the second moment of the wind stress, namely,  $\langle |w|^2 \rangle = \langle |\tau|^2 \rangle / [(f^2 + r^2) \rho_0^2]$ . This is exactly what one would expect. The long duration of constant wind stress allows the system to fully respond and adjust to the driving force, and hence, the moments of the currents are proportional to the moments of the wind stress. The coefficient of proportionality is given by the solution of eqs. (4) with constant wind stress. The other limit is when  $rT, fT \ll 1$  and, in this case,  $\langle |w|^2 \rangle \sim \langle |\tau|^2 \rangle T / (2r \rho_0^2)$ . In this limit, the second moment of the current amplitude is very small and approaching zero as the correlation time approaches zero. This result is what one would expect for a rapidly changing wind that cannot drive significant currents. The double averaged fourth moment is

$$\begin{aligned}
\overline{\langle |w|^4 \rangle} &= \frac{1}{(f^2 + r^2)^2 \rho_0^4} \left( \langle |\tau|^2 \rangle^2 g_2(T) + \langle |\tau|^4 \rangle g_4(T) \right), \\
g_2(T) &= \frac{4(D + 1 - 2A_1)}{1 - D} \left( \frac{3 - D - 2A_1 D}{4rT} - 2 \frac{3r(1 - DA_1) + fDA_2}{(f^2 + 9r^2)T} \right), \\
g_4(T) &= 1 + \frac{5 - 3D + 2A_1(A_1 - 1 - D)}{2rT} - 4 \frac{3r(1 - DA_1) + fDA_2}{(f^2 + 9r^2)T} + \frac{r(1 - A_1^2) + rA_2^2 + 2fA_1A_2 - 4r(1 - A_1) - 4fA_2}{(f^2 + r^2)T},
\end{aligned} \tag{8}$$

where  $D \equiv \exp(-2rT)$ . While at the limit  $T \rightarrow 0$  both the second and the fourth moments vanish, the ratio between them remains finite and is equal to 2. This corresponds to the Rayleigh distribution which originates in the facts that the components of the currents are independent and each has a Gaussian distribution with a zero mean and the same variance. One can easily understand the origin of the Gaussian distribution by considering the central limit theorem which can be applied in this limit. Each of the current components is the integral of many independent, identically distributed random variables (the wind stress at different times). Based on the second and fourth moments in the limit of  $T \rightarrow 0$ , we conjecture that the overall PDF of the ocean current speed, in this case, is given by the Rayleigh distribution.

*Orenstein-Uhlenbeck wind stress:* The second particular case we consider is the Orenstein-Uhlenbeck wind stress. This process results in a Gaussian wind stress with an exponentially decaying temporal correlation function. It is important to note that, due to the Gaussian nature of the force, once we have the two-point correlation function and the first two moments of the wind stress, we have all the information on the driving force. The correlation function of the wind-stress components is given by

$$\langle \tau_i(t) \tau_j(t') \rangle = \delta_{ij} \langle \tau_i^2 \rangle \exp(-\gamma_i |t - t'|). \tag{9}$$

The long time limits of the current components' averages are:

$$\langle u \rangle \sim \frac{r \langle \tau_x \rangle + f \langle \tau_y \rangle}{\rho_0 (f^2 + r^2)}, \quad \langle v \rangle \sim \frac{r \langle \tau_y \rangle - f \langle \tau_x \rangle}{\rho_0 (f^2 + r^2)}. \tag{10}$$

The long time limit of the current amplitude variance,  $s^2 \equiv \langle |w|^2 \rangle - \langle u \rangle^2 - \langle v \rangle^2$ , is given by

$$s^2 \sim \sum_{i=x,y} \frac{\langle \tau_i^2 \rangle (r + \gamma_i)}{\rho_0^2 r (f^2 + (r + \gamma_i)^2)}. \tag{11}$$

Under the assumption of isotropic wind stress, the variance may be expressed as  $s^2 \sim \langle |\tau|^2 \rangle (r + \gamma) / (\rho_0^2 r (f^2 + (r + \gamma)^2))$ . Due to the Gaussian nature of the wind stress and the

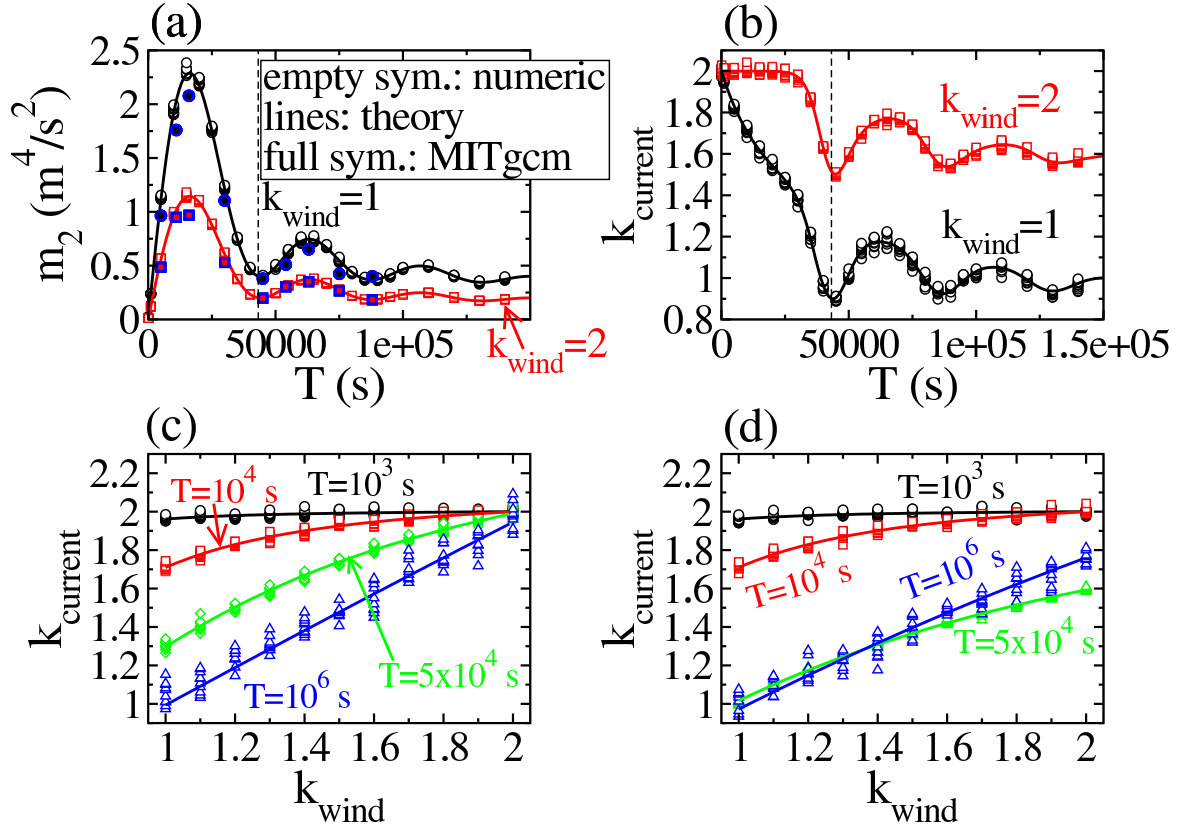


FIG. 2: (a) The second moment of the current amplitude versus the wind-stress correlation time,  $T$ . Analytical results (solid lines) compared with the numerical solution of the Ekman model (empty symbols) and the MITgcm modeling (blue symbols filled with either black or red) of the currents in a simple artificial lake. The wind stress was drawn from a Weibull distribution with two different values of the  $k_{\text{wind}}$  parameter as specified in the figure. (b) The Weibull  $k_{\text{current}}$  parameter of the current distribution versus the constant wind-stress duration. (c) The Weibull  $k_{\text{current}}$  parameter of the current distribution versus the  $k_{\text{wind}}$  parameter of the wind-stress distribution. The Coriolis parameter,  $f$ , in this case, is 0, corresponding to its value at the equator. (d) Same as panel (c) but  $f$ , in this case, is finite (corresponding to its value at the pole) and larger than  $r$ . In all panels, we had set  $r = 10^{-5} \text{s}^{-1}$ ; the results of ten realizations of the numerical solution (empty symbols) are shown for each value of  $T$  or  $k_{\text{wind}}$ . The vertical dashed line in panels (a) and (b) indicates the time period associated with the Coriolis frequency at the pole.

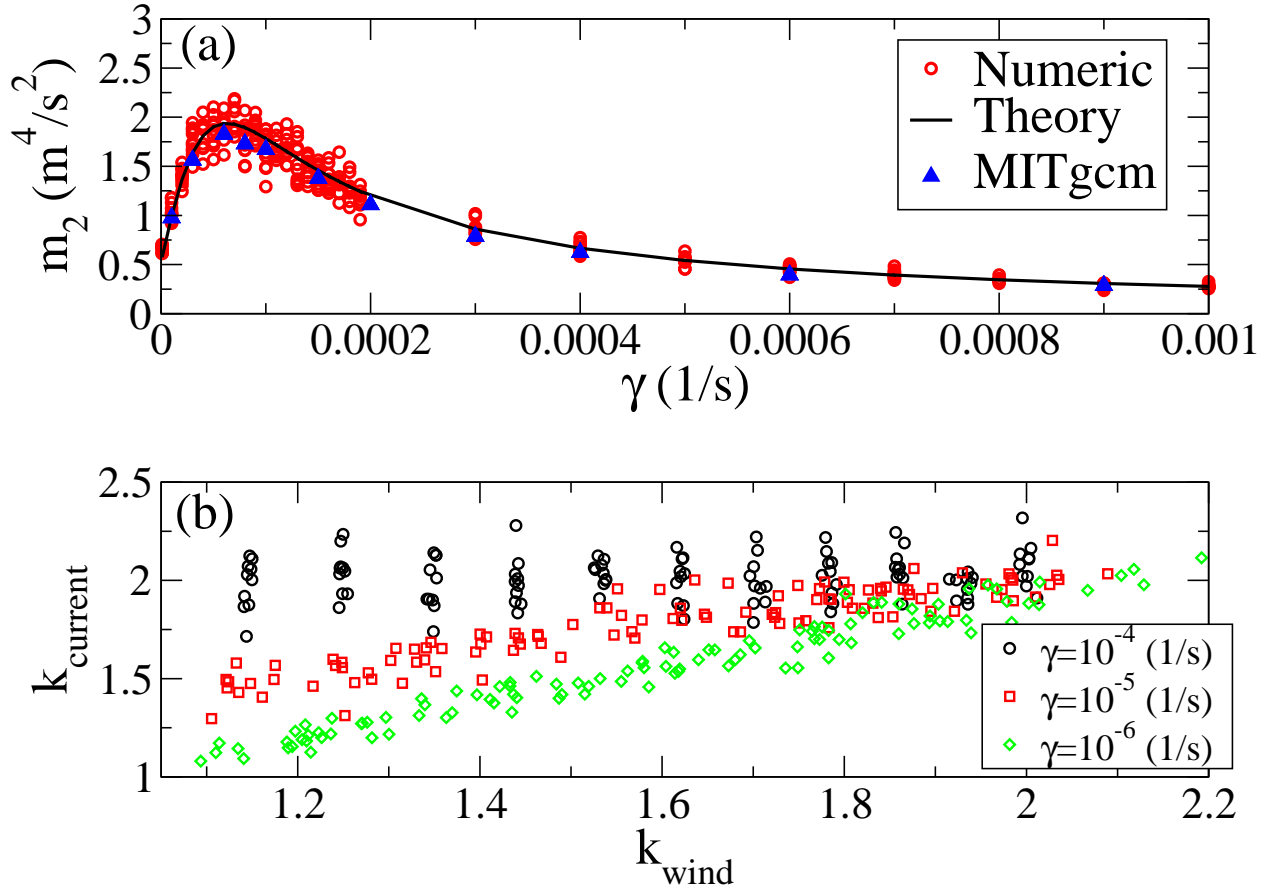


FIG. 3: (a) Comparison between the second moment of the current amplitude as calculated analytically (solid line), numerically (red circles) and by the MITgcm model (blue triangles) in a simple lake. The wind-stress amplitude was drawn from a Weibull distribution with  $k_{\text{wind}} = 1.5$ . (b) The Weibull  $k_{\text{current}}$  parameter of the current amplitude distribution versus the  $k_{\text{wind}}$  parameter of the wind stress for different correlation times. In both panels, the Coriolis parameter,  $f$ , corresponds to its value at  $\text{lat} = 30^\circ$  and  $r = 10^{-5} \text{s}^{-1}$ .

linearity of the model, the current components have Gaussian distributions which are fully characterized by the mean and variance. Note that the result of eq. (11) holds for any distribution of the wind-stress components as long as the two-point correlation function is given by eq. (9). It is clear, similar to the first idealized case discussed above, that the second moment vanishes at the limit of a short wind-stress correlation time, ( $\gamma \gg r$  and  $\gamma \gg f$ ).

*Test on detailed GCM model:* We performed two types of numerical simulations to validate the analytical derivations presented above. The first type was a simple integration of eqs. (4). As for the second type, we used a state-of-the-art oceanic GCM, the MITgcm [15], to test the applicability of our analytical derivations when the spatial variability of the bottom topography and the

nonlinearity of the ocean dynamics [11] are taken into account. We considered a 2D parabolic basin with a maximum depth of  $90m$  that is situated in a plateau of a depth of  $100m$ . The boundaries of the domain are open, and a grid with  $50 \times 50$  points and a resolution of  $1km$  is assigned. The integration time step is  $10s$ , and the overall integration time is two years. As shown in the figures, these simulations exhibited close similarity with the analytical derivations, suggesting that these may also be relevant to more realistic cases, in the presence of bottom topography and nonlinearities. We also performed similar simulations with closed boundaries and with a 10 times coarser spatial resolution; we obtained similar results in the center of the domain but not close to the periphery, suggesting that our derivations may be valid in the open ocean but not close to the shores.

*Discussion and Summary:* The results presented above highlight the important role played by the temporal correlations of the wind stress in determining the statistics of surface ocean currents. The behavior at the limits of long-range temporal correlations ( $rT \gg 1$ ) and short-range temporal correlations ( $T \rightarrow 0$ ) are intuitive, once derived. The existence of an optimal correlation time, at which the average current amplitude is maximal, is less trivial.

In Fig. 2(a), we show the second moment of the current amplitude for the isotropic, step-like wind-stress model. The analytical results (eq. (7)) are compared with the numerical solution of the Ekman model (eqs. (4)) and the MITgcm modeling of the currents in a simple artificial lake (details of which are provided above). One can see that the dependence of the average current amplitude on the constant wind-stress duration is nonmonotonic (due to the fact that the Coriolis effect is significant –  $|f| > r$ ) and that there is an excellent agreement between all the results. At the equator, where  $f = 0$ , the second moment increases monotonically to  $\langle |\tau|^2 \rangle / (r^2 \rho_0^2)$  as a function of  $T$ .

It was previously argued that, under certain conditions, the wind amplitude (directly related to the wind stress) PDF is well approximated by the Weibull distribution [3]; we thus choose, in our demonstrations, a Weibull distribution of wind stress. In Fig. 2(b), we present the Weibull  $k_{\text{current}}$  parameter [9] of the current distribution versus the constant wind-stress duration for two different values ( $k_{\text{wind}} = 1$  and  $k_{\text{wind}} = 2$ ) of the wind-stress Weibull  $k_{\text{wind}}$  parameter (again, we only present here the results of the isotropic case). One can see that, for short correlation times, the current amplitude exhibits a Rayleigh distribution ( $k_{\text{current}} = 2$ ), independent of the wind-stress distribution. This corresponds to Gaussian distributions of the current components. In the other limit of long constant wind-stress periods,  $k_{\text{current}}$  converges to  $k_{\text{wind}}$  (not shown for  $k_{\text{wind}} = 2$ ).

The above results were obtained for the maximal value of the Coriolis parameter, i.e.,  $f$  at the pole. In Fig. 2(c,d) we show  $k_{\text{current}}$  versus  $k_{\text{wind}}$  for different values of the constant wind-stress duration,  $T$ , and the two limiting values of the Coriolis parameter,  $f$ , at the equator and at the pole. Here again, one observes an excellent agreement between the numerical and the analytical results for both values of  $f$ . The limits of short and long temporal correlations of the wind, at which  $k_{\text{current}} = 2$  and  $k_{\text{current}} = k_{\text{wind}}$ , correspondingly, are clearly demonstrated.

In Fig. 3, we present similar results for the case of an exponentially decaying correlation function of the wind stress. In Fig. 3(a), we present the second moment of the current amplitude versus the decay rate of the correlation function. The existence of an optimal decay rate, for which the average current amplitude is maximal, is demonstrated for this case as well. One notable difference is the absence of the secondary maxima points which appeared in the step-like model. For this case, one may easily find that the maximal average amplitude of the currents is obtained for  $\gamma = |f| - r$ , assuming that  $|f| \geq r$ . In Fig. 3(b), we present  $k_{\text{current}}$  versus  $k_{\text{wind}}$ . Here again, we obtain an excellent agreement between the predicted and the numerically obtained limiting behaviors. It is important to note that the good agreement between the MITgcm results and the analytical results has been proven to be valid only for the setup described above. Different behavior may occur for different scenarios such as regions close to the boundary of the domain, spatially variable wind, complex and steep bottom topography, and vertically and spatially variable temperature and salinity. Close to the boundaries of the artificial lake, the results showed a significant deviation due to the boundary effects that were neglected in the analytical model. Moreover, we used a spatially uniform wind stress in our simulation and have not considered the more realistic case of non-uniform wind stress.

In summary, we have shown, in two idealized cases, that the PDF of wind-driven ocean currents depends on the temporal correlations of the wind. For short-range correlations, the current speed approaches zero, and the PDF of its components is Gaussian. For long-range temporal correlations of the wind, the currents' PDF is proportional to the wind-stress PDF. The model we used highly simplifies real ocean dynamics, yet our numerical results suggest that, qualitatively, the above conclusions should also be valid in more general, realistic cases. Analysis that is based on the space dependent model (either in the horizontal or the vertical dimensions or both) is a natural extension of the current study and will allow us to compare the analytical results to altimetry-based surface currents and to study non-local phenomena.

---

\* Electronic address: `bel@bgu.ac.il`

† Electronic address: `ashkena@bgu.ac.il`

- [1] J. V. Seguro and T. W. Lambert, *J. Wind Engineering and Industrial Aerodynamics* **85**, 75 (2000).
- [2] A. H. Monahan, *J. Climate* **19**, 497 (2006).
- [3] A. H. Monahan, *J. Climate* **23**, 5151 (2010).
- [4] P. C. Chu, *Geophys. Res. Lett.* **35**, L12606 (2008).
- [5] S. T. Gille and S. G. L. Smith, *Phys. Rev. Lett.* **81**, 5249 (1998).
- [6] S. T. Gille and S. G. L. Smith, *J. Phys. Oceanogr.* **30**, 125 (2000).
- [7] P. C. Chu, *IEEE J. of Selected Topics in Applied Earth Observations and Remote Sensing* **2**, 27 (2009).
- [8] Y. Ashkenazy and H. Gildor, *J. Phys. Oceanogr.* p. in press (2011).
- [9] The Weibull distribution is characterized by two parameters,  $k$  and  $\lambda$ , and is given by  $W_{k,\lambda}(x) = \frac{k}{\lambda} \left(\frac{x}{\lambda}\right)^{k-1} \exp\left(-\left(x/\lambda\right)^k\right)$ .
- [10] V. W. Ekman, *Arch. Math. Astron. Phys.* **2**, 1 (1905).
- [11] A. E. Gill, *Atmosphere–ocean dynamics* (Academic Press, London, 1982).
- [12] B. Cushman-Roisin, *Introduction to geophysical fluid dynamics* (Prentice Hall, 1994), 1st ed.
- [13] E. Kalnay, M. Kanamitsu, R. Kistler, W. Collins, D. Deaven, L. Gandin, M. Iredell, S. Saha, G. White, J. Woollen, et al., *Bulletin of the American Meteorological Society* **77**, 437 (1996).
- [14] T. J. Simons, *Can. Bull. Fish. Aquat. Sci.* **203**, 68 (1980).
- [15] MITgcm Group, Online documentation, MIT/EAPS, Cambridge, MA 02139, USA (2010), [http://mitgcm.org/public/r2\\_manual/latest/online\\_documents/manual.html](http://mitgcm.org/public/r2_manual/latest/online_documents/manual.html).